Problemy Matematyczne
14 (1995), 127 - 147

# Mathematical and physical parameters of extinction curves originated in single interstellar cloud

Walter Wegner  Jacek Papaj

## 1. Introduction

The interstellar extinction of starlight (observed in the form of voids in the background of faint stars) is the most spectacular phenomenon revealing the presence of diffuse dark matter in the Galaxy. The extinction is commonly believed to be caused by grains of interstellar dust. Their physical and geometrical properties are thus responsible for the wavelength dependence of interstellar extinction – the extinction curve. The extinction curve certainly contains information about chemical composition, crystalline structure and other properties of the interstellar dust particles. The observed great variety of extinction curves makes necessary the determination of some objective criteria to facilitate the disussion of similarities and differences between individual extinction curves. The another reason for determining such criteria is the investigation of relations between the shape of extinction curve and some other parameters of interstellar grains such as chemical compositions, shape and size distributions.

First attempts to parametrize the extinction curve in the extraterrestrial ultraviolet are these of Savage (1975). He found the Lorentz profile as a good approximation of the prominent 2200Å feature. Seaton (1979) used the

same profile to approximate his mean extinction curve. However, using a combination of Lorentz function with polynomials of first and second degree he introduced many independent parameters. Carnochan (1986) analyzing the spectra of TD-1 satellite reduced the number of the necessary parameters to three using also the Lorentz profile. Another function has been proposed by Fitzpatrick and Massa (1986). They divided the spectral range into two parts, using a different function in every of them. The far-UV term of their function so called "Drude profile" allows to approximate the observational data more precisely than the Lorentz one. Also the physical interpretation of the derived parameters is more straightforward. Fitzpatrick and Massa (1988) introduced an additional higher order term to facilitate the fitting. Basing on this proposition Cardelli *et al.* (1989) introduced the following formula:

$$\frac{A_\lambda}{A_V} = a(\lambda^{-1}) + \frac{b(\lambda^{-1})}{\mathbf{R}}, \tag{1}$$

in which $a(\lambda^{-1})$ and $b(\lambda^{-1})$ are the two terms, empirically determined for different spectral ranges.

There are several theories that explain the shape of the extinction law caused by the interstellar grains with different chemical composition, shape and size.

1. bare silicate/graphite grains — Draine and Lee (1984), Mathis, Rumpl and Nordsieck (1977) (MRN)
2. core/mantle grains — Greenberg (1989)
3. silicate cores with amorphous carbon mantles — Duley *et al.* (1989)
4. composite grains — Mathis and Whiffen (1989), Tilens (1989)
5. fractal grains — Wright (1987)
6. biological grains — Wallis, M.K. *et al.* (1989)

All of the theories can probably explain the observed extinction in general terms, but certain crucial observations, such as the wavelength behaviour extinction in the wavelength range near the strong silicate absorption bands, will probably be able to favour bare silicate/graphite theory (Mathis 1989).

In this paper we are using MRN model, which can be simply compared with observations.

## 2. The observational material and the method of reduction

The great majority of observationally determined extinction curves — Aiello *et al.* (1988), Fitzpatrick and Massa (1990) — concern however, relatively distant, heavily reddened objects. Such objects are very likely to be obscured by several interstellar clouds situated along the same line of sight, differing in their physical parameters and/or dust content (Krełowski and Wegner 1990). The extinction curves derived from their spectra are ill-defined averages over all observed clouds and therefore - useless as a source of information concerning physical parameters of dust particles contained in any of them. Slightly reddened stars are most likely to be obscured by single clouds being quite homogeneous media. We accept however that low reddening does not prove that a star is obscured by a single cloud but the probability of this situation is higher when reddening is lower. We selected several examples of extinction curves (called "Zeta","Sigma" and "Upsilon" families – see Krełowski and Wegner 1989) from the atlas of Papaj, Wegner and Krełowski (1991). Their primary data are listed in Table 1 - see also Wegner, Papaj and Krełowski (1991). The interstellar absorption in their spectra were proved to be dominated by single interstellar clouds in cases of HD's: 144217,145502 and 147165 - by Westerlund and Krełowski (1988); in the case of 147933 - by Danks et al. (1984); in the case of HD's 23180, 149757, and 224572 - by Hobbs (1974,1978); and in the case of HD 202904 - by Hobbs (1969). In other cases, low reddening suggests that single cloud obscuration is more probable than a combination of several clouds. At least in the case of HD 44458 no Doppler splitting has been found in the profiles of diffuse interstellar bands (Porceddu,Benvenuti and Krełowski 1991).

One of possible ways of analyzing the extinction curves consists of fitting an analytical forlmula to the observational points. We have tried to fit the above extinction curves in the UV spectral range using the formula proposed by Fitzpatrick and Massa (1986):

$$F_D(\lambda^{-1}; a_1, a_2, A, \lambda_0, \gamma) = a_1 + a_2\lambda^{-1} + \frac{A}{\left[\lambda^{-1} - \left(\lambda_0^{-1}\right)^2/\lambda^{-1}\right]^2 + \gamma^2}. \quad (2)$$

The $F_D(\lambda^{-1}; a_1, a_2, A, \lambda_0, \gamma)$ function fits quite well varied extinction curves assiging to them sets of precisely determined quantitative parameters. On Figures 1 — 10 are shown the coparisons of the UV extinction curves calculated with the (2) formulae with those determined observationally.

The available observational material also consists of photometric data from ANS UV observations (Wesselius *et al.* 1982), the additional basic parameters such as UBV magnitudes or spectral types and luminosity classes are taken from *The Bright Star Catalogue*, Hoffleit and Jaschek (1982). The extinction values, which are given in Table 2, have been derived using artificial standards from Papaj, Krełowski and Wegner (1993). For HD 23180 and HD 149757 extinction values have been obtained with "pair method" and standards from Wegner, Papaj and Krełowski (1991).

The original MRN model assumes that distributions of the silicate and graphite grains have the same parameters. In our aproach each dust constituent is characterized by power-law distribution of grain radii $a$:

$$n_i(a) = A_i n_H a^{-p}; \qquad for \qquad a_i^- \leq a \leq a_i^+ \tag{3}$$

normalized in such way, that the integral $\int_{a_i^-}^{a_i^+} n_i(a)da$ is equal to the total number density of particles of type "i" with radii in the interval $[a_i^-, a_i^+]$. Here, $n_H$ is the number density of H nuclei and "i" can be equal to "C" (for graphite) or "Si" (for silicate grains).

## 3. Results and discussion

Parameters for stars included in our programme are listed in Table 3. It gives HD number, slope and intercept ($a_2$ and $a_1$), height of a bump ($A$), the bump central wavelength ($1/\lambda_0$), bump width parametr ($\gamma$), total to selective extinction ratio ($R_{UV}$), difference between the largest and the least grain size ($da = a_i^+ - a_i^-$) and the power-law index ($p$) — equation (3). $R_{UV}$ is calculated from parameters of MRN models attained for the best consistency with observational values of extinction. Let's consider possible relations between these parameters. The two parameters, describing the linear term of the profile — $a_1$ and $a_2$ — correlate apparently very tightly (Fig. 12). The slope of the linear term in the profile is thus very important parameter dividing the extinction curves into families. Fig. 13, 14 and 15

show the evident differences of parameters describing the 3 "families" being considered in this paper.

Acknowledgments. This project has been supported partially by the Nicolaus Copernicus University under the grant 683-A.

# References

[1] Aiello S., Barsella B., Chlewicki G., Greenberg J.M., Patriarchi P., Perinotto M., 1988 *Astron. Astrophys. Suppl. Ser.* **73**, 195.

[2] Cardelli J.A., Clayton G.C., Mathis. J.S., 1989 *Astrophys. J.* **345**, 245.

[3] Carnochan D.J., 1986 *Mon. Not. R. Astron. Soc.* **219**, 903.

[4] Danks A.C.,Federman S.R., Lambert.D.L.,1984 *Astron.Astrophys.* **130**,62.

[5] Draine B.T., Lee H.N., 1984 *Astrophys. J.* **285**, 89.

[6] Duley W.W., Jones A.P., Williams D.A., 1989 *Mon. Not. R. Astron. Soc.* **236**, 709.

[7] Fitzpatrick E.L., Massa D., 1986 *Astrophys. J.* **307**, 286.

[8] Fitzpatrick E.L., Massa D., 1988 *Astrophys. J.* **328**, 734.

[9] Fitzpatrick E.L., Massa D., 1990 *Astrophys. J. Suppl. Ser.* **72**, 163.

[10] Greenberg J.M., 1989 in *Highlights of Astronomy*, ed. D. McNally, **8**, 241, Dordrecht, Kluwer.

[11] Hobbs L.M., 1969 *Astrophys. J.* **157**, 135.

[12] Hobbs L.M., 1974 *Astrophys. J.* **191**, 381.

[13] Hobbs L.M., 1978 *Astrophys. J. Suppl.* **38**, 129.

[14] Hoffleit D., Jaschek C., 1982 *The Bright Star Catalogue*, Yale University Observatory, New Haven.

[15] Krełowski J., Wegner W., 1989 *Astron. Nachr.* **310** 281.

[16] Mathis J.S., 1989, in *Interstellar dust*, IAU Symp. No. 135, Dordrecht, Kluwer, p.357.

[17] Mathis J.S., Rumpl W., Nordsieck K.H., 1977 *Astrophys. J.* **217**, 425 — MRN.

[18] Mathis J.S., Whiffen G., 1989 *Astrophys. J.* **341**, 808.

[19] Papaj J., Krełowski J., Wegner W., 1993 *Astron. Astrophys* — in press.

[20] Papaj J., Wegner W., Krełowski J., 1991 *Mon. Not. R. Astron. Soc.* **252**, 403.

[21] Porceddu I..Benvenuti P. and Krełowski J..1991 *Astron.Astrophys.* submitted

[22] Savage B.D., 1975 *Astrophys. J.* **199**, 92.

[23] Seaton M.J., 1979 *Mon. Not. R. Astron. Soc.* **187**, 73p.

[24] Tielens A.G.G.M., 1989, in *Interstellar dust*, IAU Symp. No. 135, Dordrecht, Kluwer, p.239.

[25] Wallis M.K., Wickramasinghe N.C., Hoyle, F., Rabilizirov, R., 1989, *Mon. Not. R. Astron. Soc.* **238**, 1165.

[26] Wegner W., Papaj J., Krelowski J., 1991, *Acta Astron.* **41**, 149.

[27] Wesselius P.R., van Duinen R.J., de Jonge A.R.W., Aalders, J.W.G., Luinge W., Wildeman K.J., 1982 *Astron. Astrophys. Suppl. Ser.* **49**, 427.

[28] Westerlund B.E. and Krełowski J.,1988.*Astron.Astrophys.* **189**,221.

[29] Wright E.L., 1987 *Astrophys. J.* **320**, 818.

PEDAGOGICAL UNIVERSITY
INSTITUTE OF MATHEMATICS
Chodkiewicza 30
85-064 Bydgoszcz
Poland

N. COPERNICUS UNIVERSITY
INSTITUTE OF ASTRONOMY
Chopina 12/18
87-100 Toruń
Poland

**Table 1. Primary data for the target stars.**

| HD | Sp/L | MK | B-V | E(B-V) |
|---|---|---|---|---|
| zeta family | | | | |
| 23180 | B1 III | B1 III | 0.05 | 0.26 |
| 149757 | O9.5 V | O9.5 Vn | 0.02 | 0.29 |
| 224572 | B1 V | B1 V | -0.07 | 0.16 |
| sigma family | | | | |
| 144217 | B0.5 V | B1 V | -0.07 | 0.17 |
| 145502 | B1 V | B3 V | 0.04 | 0.27 |
| 147165 | B1 III | B2 III + O9.5 V | 0.13 | 0.34 |
| 147933 | B2 V | B2 IV | 0.24 | 0.45 |
| upsilon family | | | | |
| 44458 | B1 V | B1 Vpe | -0.02 | 0.21 |
| 30076 | B1.5 V | B2 Ve | -0.11 | 0.10 |
| 202904 | B0.5 V | B2 Vne | -0.11 | 0.13 |

**Table 2. The extinction data for the target stars.**

| HD | $k_V$ | $k_B$ | $k_U$ | $k_{33}$ | $k_{25}$ | $k_{22}$ | $k_{18}$ | $k_{155}$ |
|---|---|---|---|---|---|---|---|---|
| 23180 | 0.0 | 1.0 | 1.73 | 3.25 | 4.21 | 6.61 | 4.57 | 4.74 |
| 149757 | 0.0 | 1.0 | 1.34 | 3.15 | 4.08 | 6.07 | 4.87 | 5.36 |
| 224572 | 0.0 | 1.0 | 1.75 | 2.31 | 4.56 | 7.08 | 4.81 | 4.81 |
| 144217 | 0.0 | 1.0 | 1.77 | 1.84 | 3.70 | 6.01 | 3.48 | 3.72 |
| 145502 | 0.0 | 1.0 | 2.07 | 2.11 | 4.11 | 6.67 | 3.63 | 3.15 |
| 147165 | 0.0 | 1.0 | 1.75 | 2.09 | 3.79 | 5.88 | 3.44 | 2.97 |
| 147933 | 0.0 | 1.0 | 1.49 | 1.58 | 3.11 | 5.11 | 2.73 | 2.42 |
| 44458 | 0.0 | 1.0 | 1.43 | 1.67 | 3.95 | 5.67 | 7.42 | 5.76 |
| 30076 | 0.0 | 1.0 | 1.50 | 3.30 | 6.20 | 8.10 | 8.20 | 8.90 |
| 202904 | 0.0 | 1.0 | 2.38 | 2.46 | 5.73 | 7.15 | 7.69 | 8.08 |

Table 3. Mathematical and physical extinction parameters of the stars.

| HD | $a_1$ | $a_2$ | A | $1/\lambda_0$ | $\gamma$ | $A/\gamma$ | $R_{UV}$ | da | p |
|---|---|---|---|---|---|---|---|---|---|
| 23180 | -4.482 | 0.836 | 6.576 | 4.586 | 1.250 | 5.26 | 3.95 | 0.265 | 3.405 |
| 149757 | -3.803 | 0.889 | 3.001 | 4.569 | 1.049 | 2.86 | 3.95 | 0.275 | 3.370 |
| 224572 | -3.393 | 0.810 | 3.170 | 4.584 | 0.926 | 3.42 | 3.90 | 0.271 | 3.479 |
| 144217 | -2.023 | 0.361 | 2.636 | 4.568 | 0.794 | 3.32 | 4.80 | 0.269 | 3.192 |
| 145502 | -1.247 | 0.159 | 2.897 | 4.549 | 0.834 | 3.47 | 4.65 | 0.257 | 3.282 |
| 147165 | -1.112 | 0.122 | 3.221 | 4.570 | 0.923 | 3.49 | 5.15 | 0.266 | 3.138 |
| 147933 | -1.204 | 0.145 | 2.978 | 4.567 | 0.917 | 3.25 | 6.45 | 0.277 | 2.882 |
| 44458 | -5.392 | 1.255 | 5.705 | 4.685 | 1.466 | 3.89 | 6.00 | 0.353 | 3.188 |
| 30076 | -5.395 | 1.502 | 3.477 | 4.705 | 1.277 | 2.72 | 3.75 | 0.376 | 3.790 |
| 202904 | -5.949 | 1.268 | 8.624 | 4.622 | 1.696 | 5.08 | 4.45 | 0.396 | 3.608 |

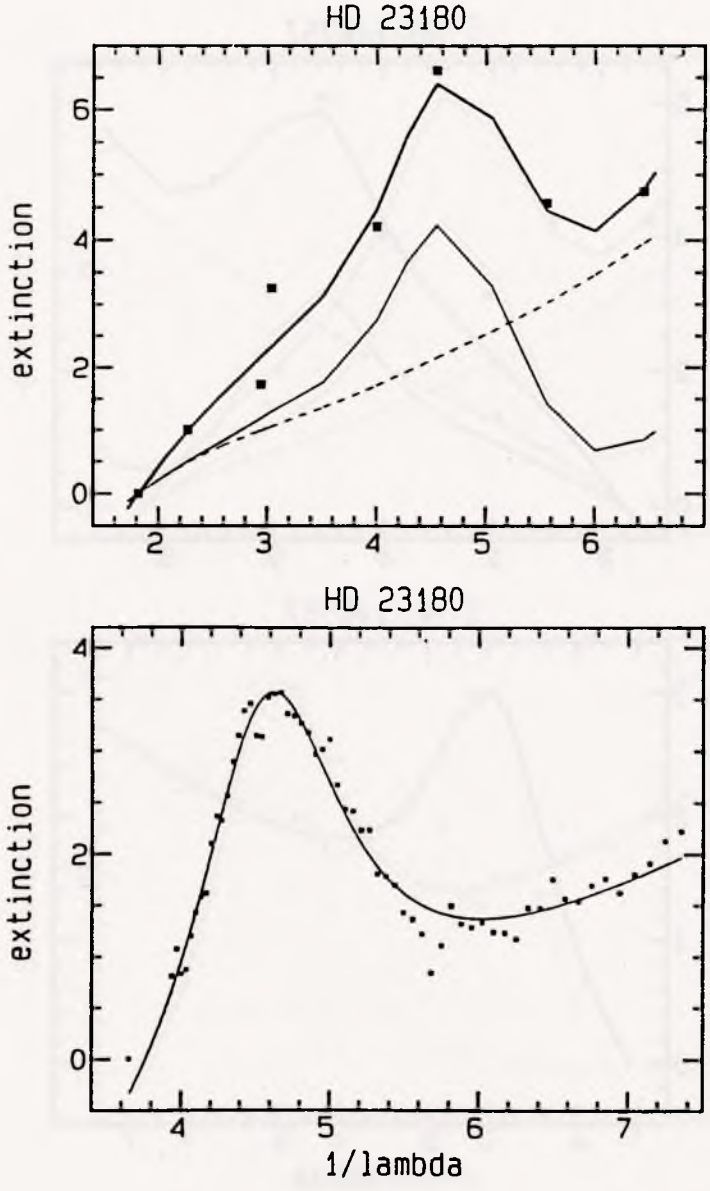


**Figure 1.**
Upper frame — the observed extinction is compared with our best fit (solid, bold line) obtained with the assumption that graphite and silicate grains can have the same size distributions. The separate contributions of silicates (dashed line) and graphites (solid line) are also shown. Lower frame — the coparison of the UV extinction curves calculated with the (2) formulae (solid lines) with those determined observationally (small dots).

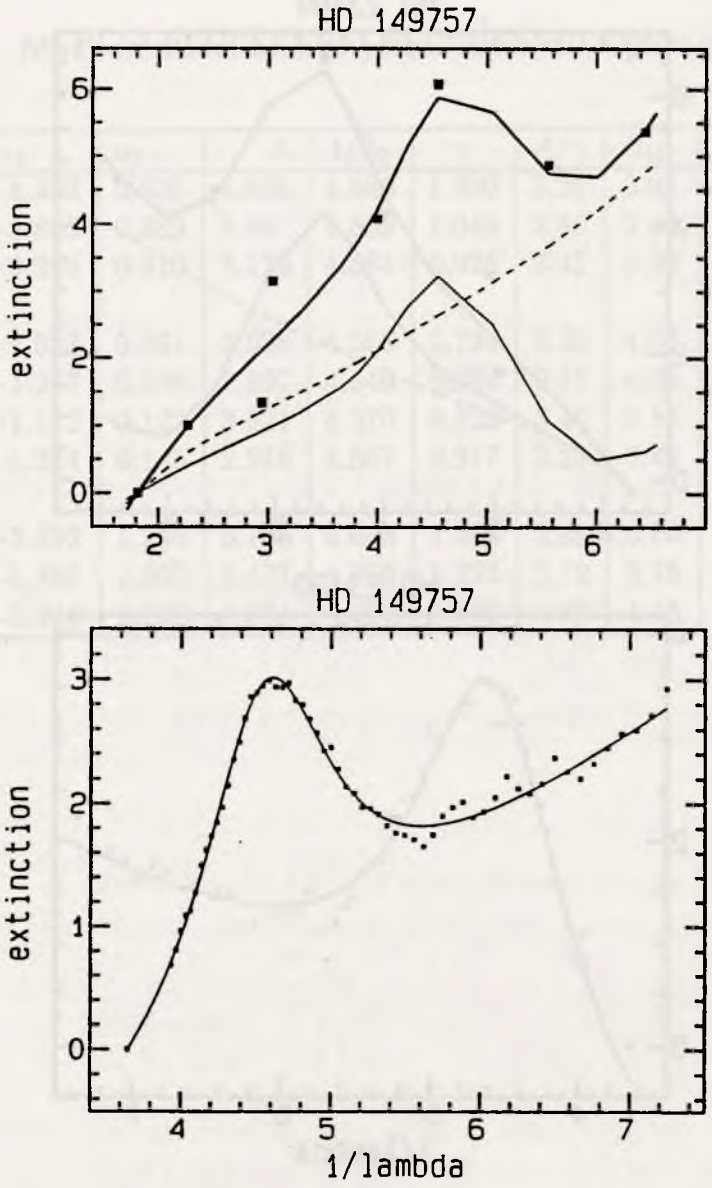


**Figure 2.**
Upper frame — the observed extinction is compared with our best fit (solid, bold line) obtained with the assumption that graphite and silicate grains can have the same size distributions. The separate contributions of silicates (dashed line) and graphites (solid line) are also shown. Lower frame — the coparison of the UV extinction curves calculated with the (2) formulae (solid lines) with those determined observationally (small dots).

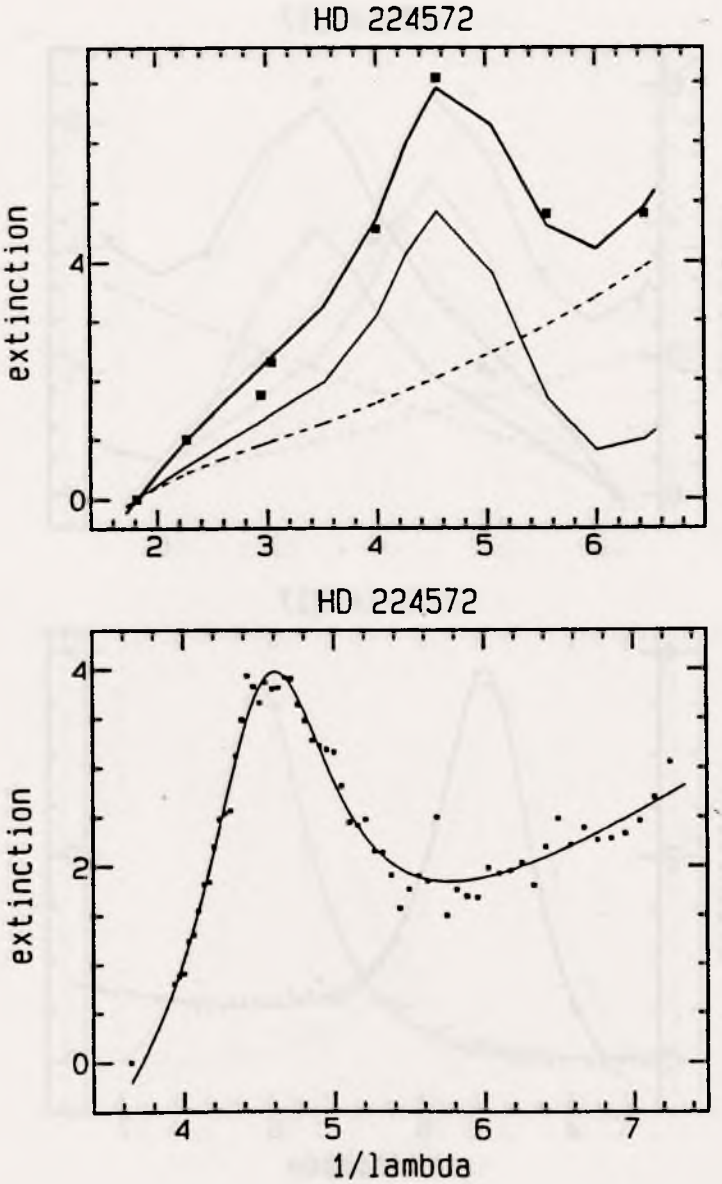


**Figure 3.**
Upper frame — the observed extinction is compared with our best fit (solid, bold line) obtained with the assumption that graphite and silicate grains can have the same size distributions. The separate contributions of silicates (dashed line) and graphites (solid line) are also shown. Lower frame — the coparison of the UV extinction curves calculated with the (2) formulae (solid lines) with those determined observationally (small dots).

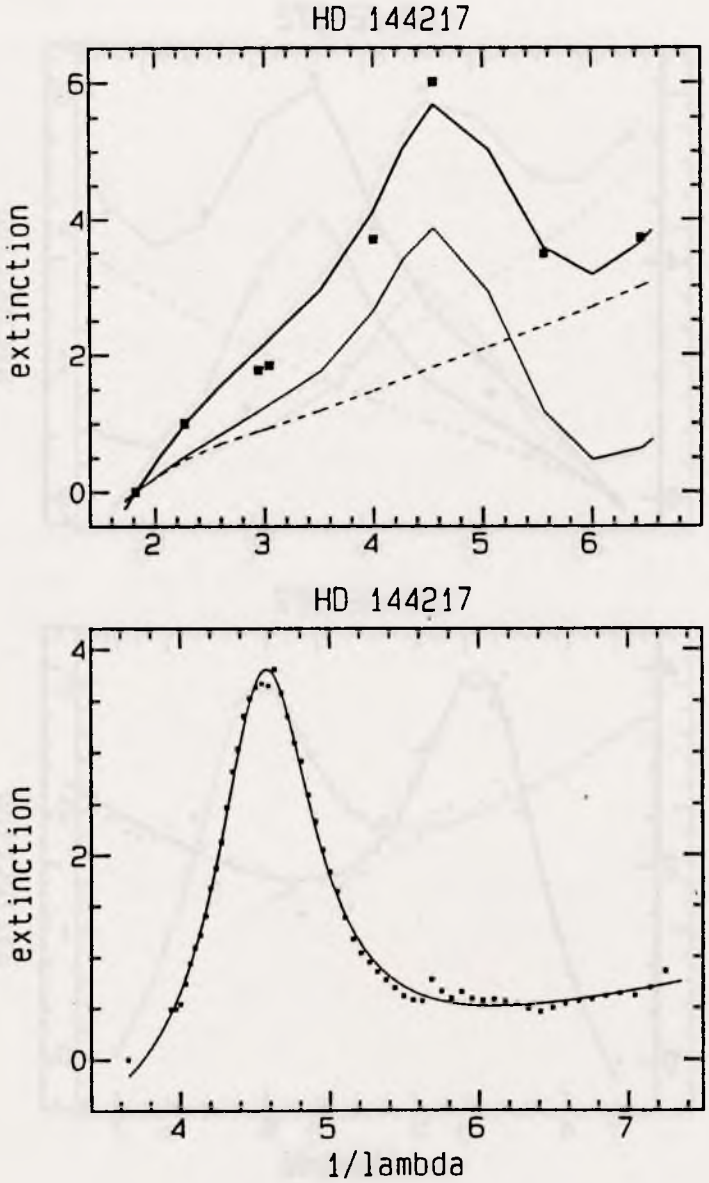


**Figure 4.**
Upper frame — the observed extinction is compared with our best fit (solid, bold line) obtained with the assumption that graphite and silicate grains can have the same size distributions. The separate contributions of silicates (dashed line) and graphites (solid line) are also shown. Lower frame — the coparison of the UV extinction curves calculated with the (2) formulae (solid lines) with those determined observationally (small dots).

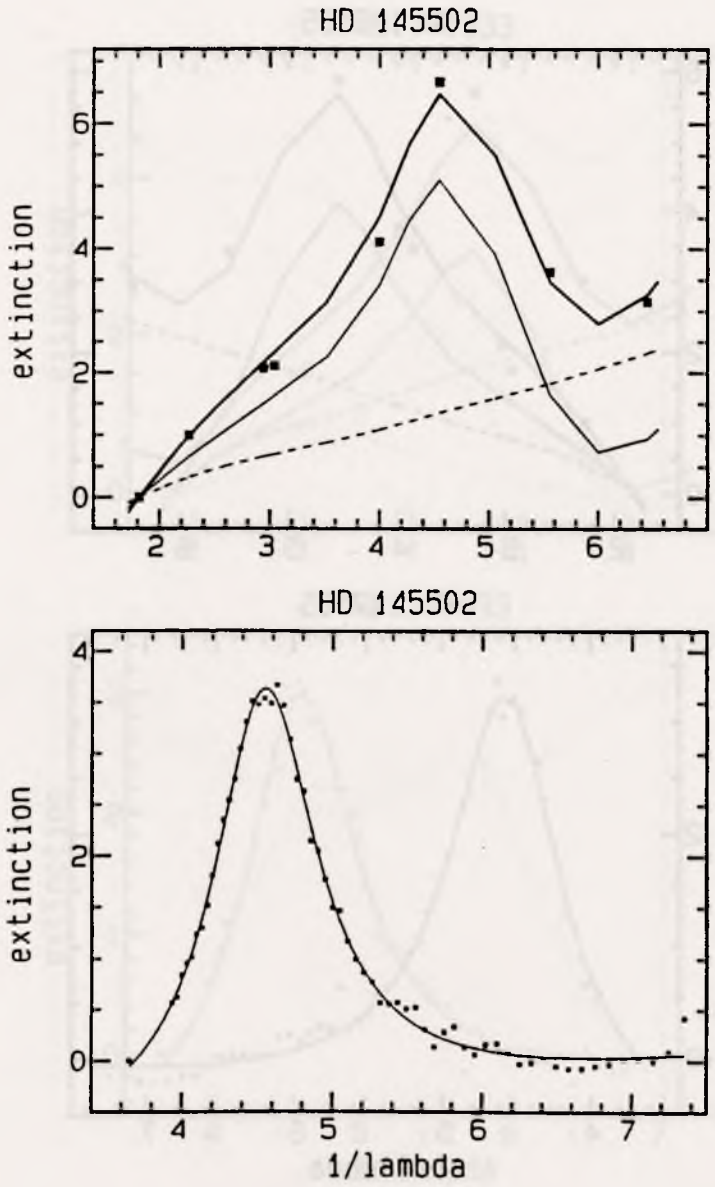


**Figure 5.**
Upper frame — the observed extinction is compared with our best fit (solid, bold line) obtained with the assumption that graphite and silicate grains can have the same size distributions. The separate contributions of silicates (dashed line) and graphites (solid line) are also shown. Lower frame — the coparison of the UV extinction curves calculated with the (2) formulae (solid lines) with those determined observationally (small dots).

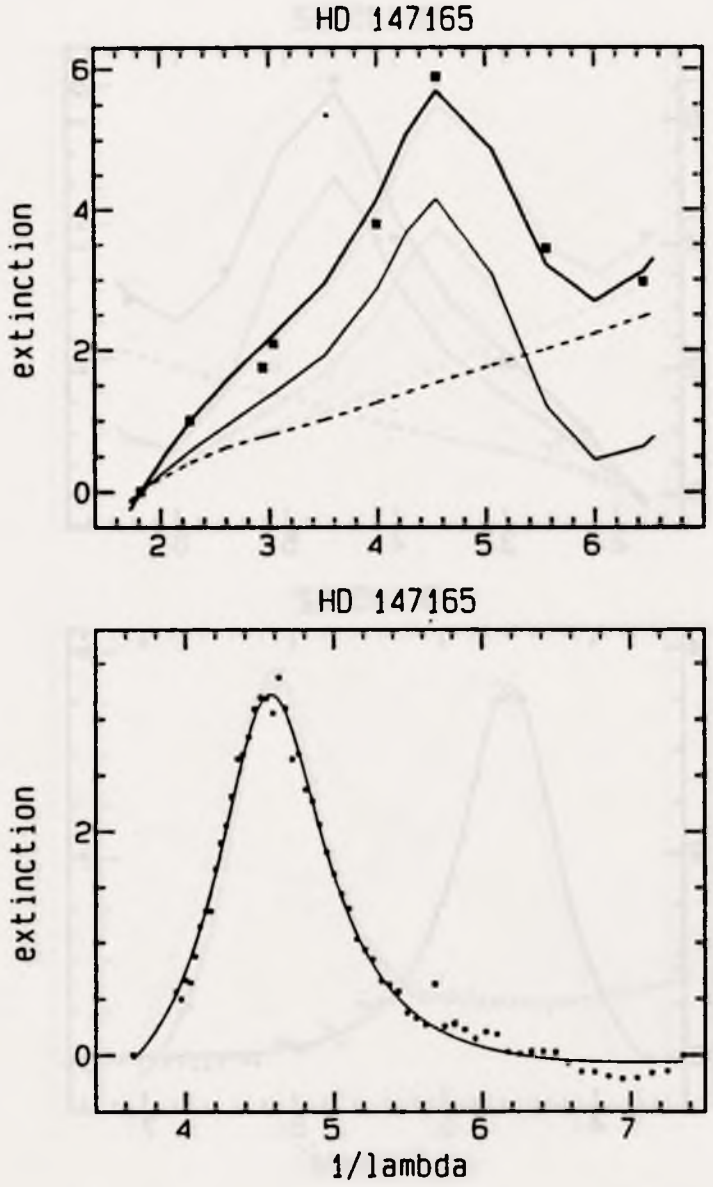


**Figure 6.**
Upper frame — the observed extinction is compared with our best fit (solid, bold line) obtained with the assumption that graphite and silicate grains can have the same size distributions. The separate contributions of silicates (dashed line) and graphites (solid line) are also shown. Lower frame — the coparison of the UV extinction curves calculated with the (2) formulae (solid lines) with those determined observationally (small dots).

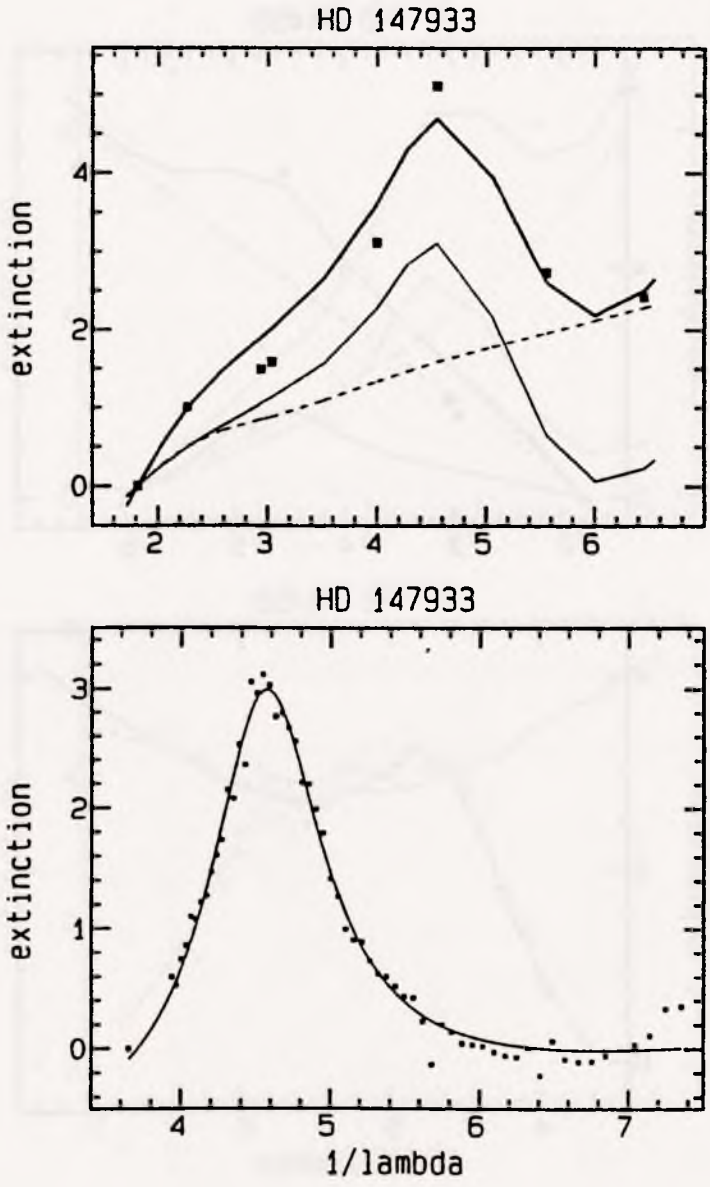


**Figure 7.**
Upper frame — the observed extinction is compared with our best fit (solid, bold line) obtained with the assumption that graphite and silicate grains can have the same size distributions. The separate contributions of silicates (dashed line) and graphites (solid line) are also shown. Lower frame — the coparison of the UV extinction curves calculated with the (2) formulae (solid lines) with those determined observationally (small dots).

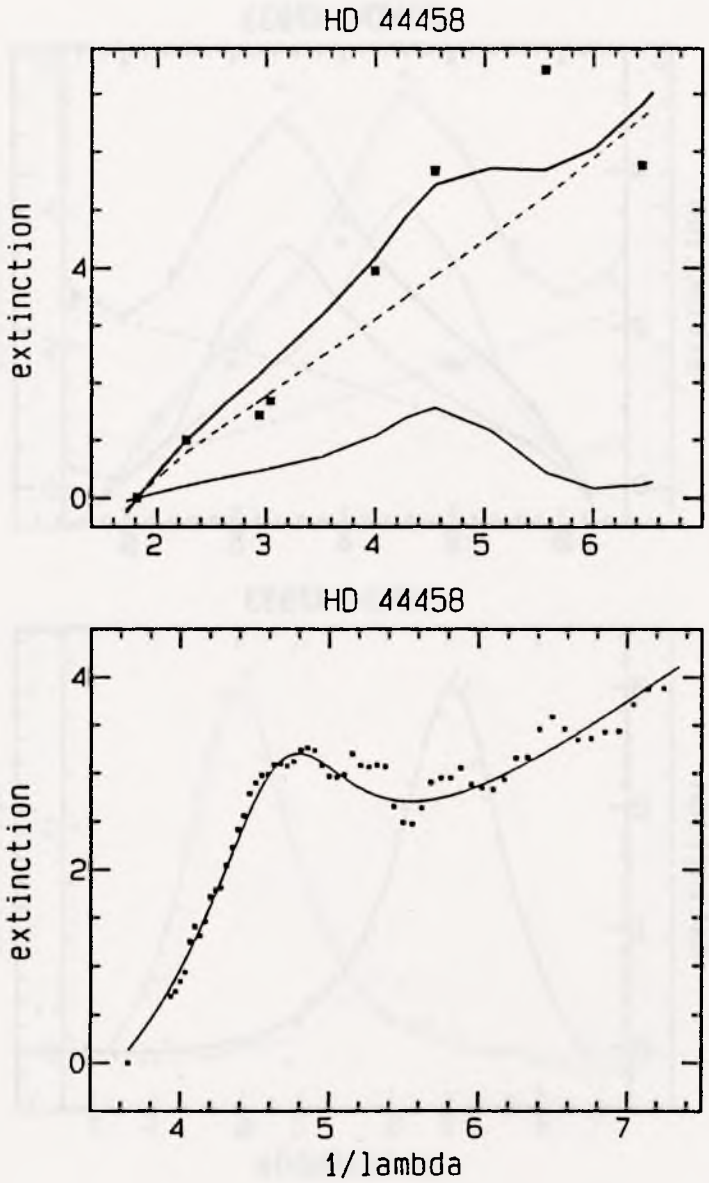


**Figure 8.**
Upper frame — the observed extinction is compared with our best fit (solid, bold line) obtained with the assumption that graphite and silicate grains can have the same size distributions. The separate contributions of silicates (dashed line) and graphites (solid line) are also shown. Lower frame — the coparison of the UV extinction curves calculated with the (2) formulae (solid lines) with those determined observationally (small dots).

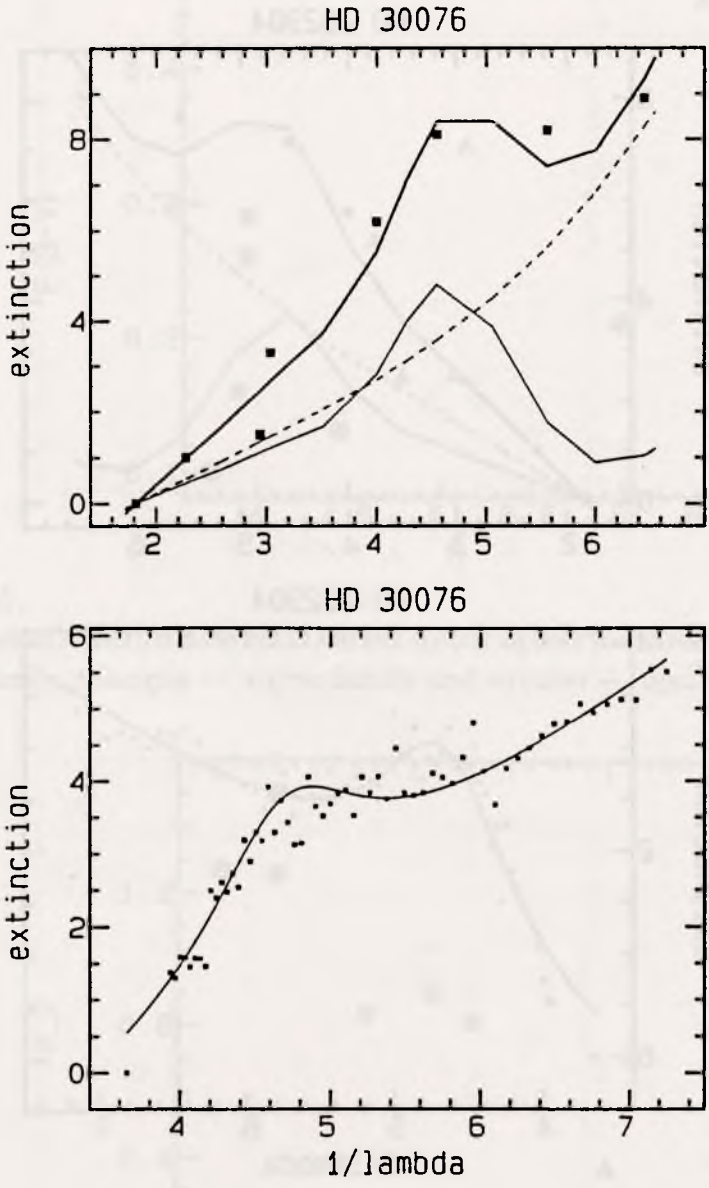


**Figure 9.**
Upper frame — the observed extinction is compared with our best fit (solid, bold line) obtained with the assumption that graphite and silicate grains can have the same size distributions. The separate contributions of silicates (dashed line) and graphites (solid line) are also shown. Lower frame — the coparison of the UV extinction curves calculated with the (2) formulae (solid lines) with those determined observationally (small dots).

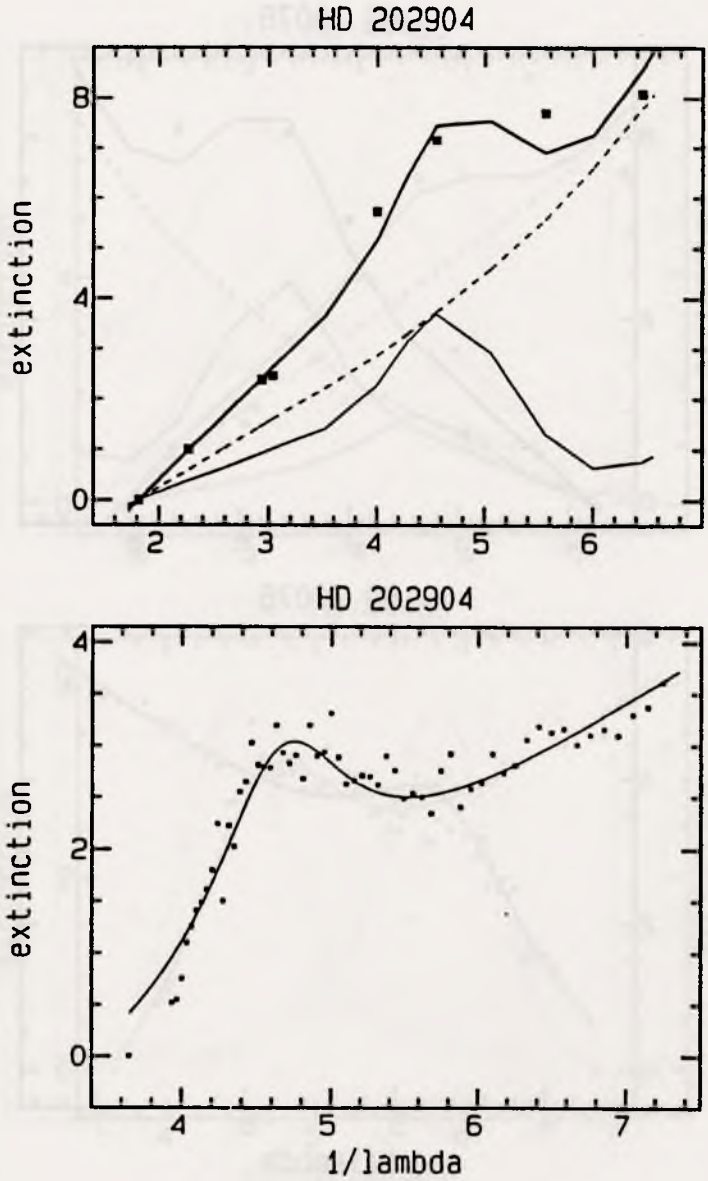


**Figure 10.**
Upper frame — the observed extinction is compared with our best fit (solid, bold line) obtained with the assumption that graphite and silicate grains can have the same size distributions. The separate contributions of silicates (dashed line) and graphites (solid line) are also shown. Lower frame — the coparison of the UV extinction curves calculated with the (2) formulae (solid lines) with those determined observationally (small dots).

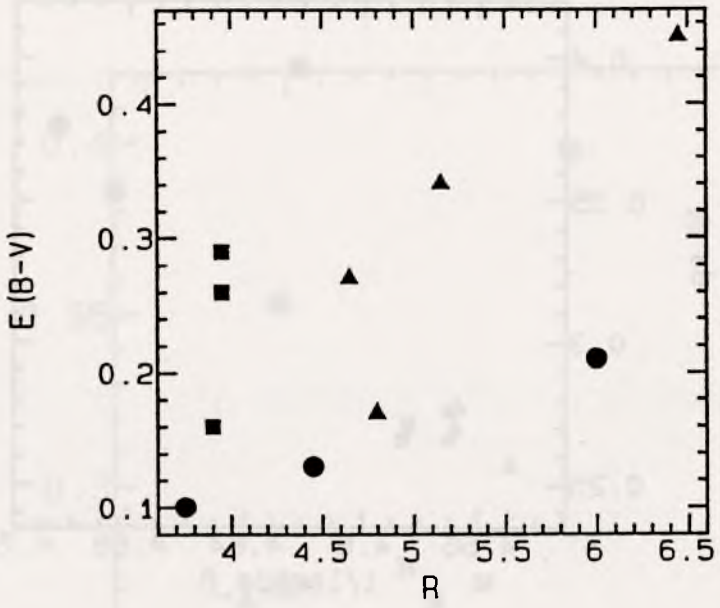


**Figure 11.**
Total to selective extinction ratio versus colour excess for three families. Dots — zeta family, triangles — sigma family and squares — upsilon family.

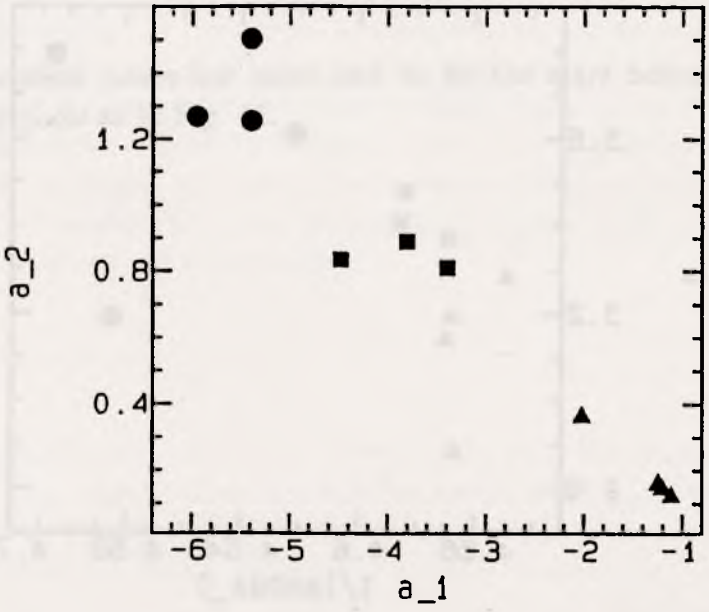


**Figure 12.**
Linear relation between $a_1$ and $a_2$ parameters for our families. Symbols as in Fig. 11.

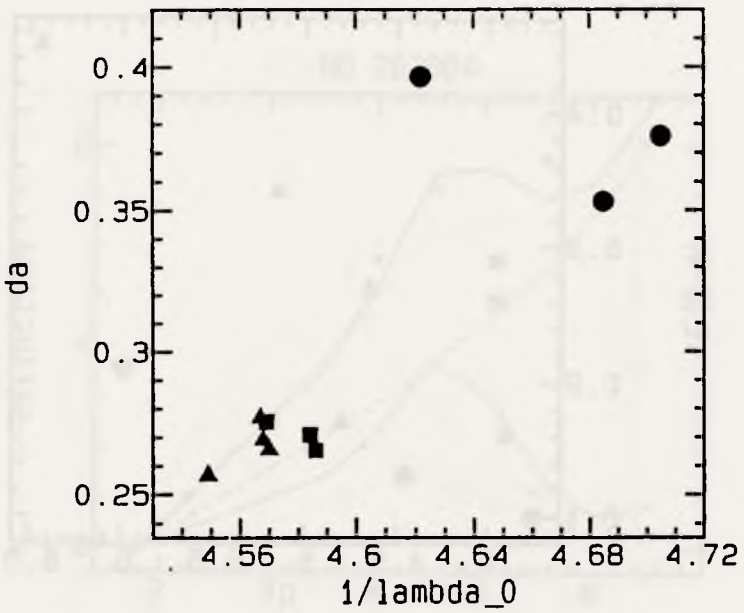


**Figure 13.**
Position of the central wavelength $\lambda_0$ of the 2200Åbump is plotted versus *da*. Symbols as in Fig. 11.

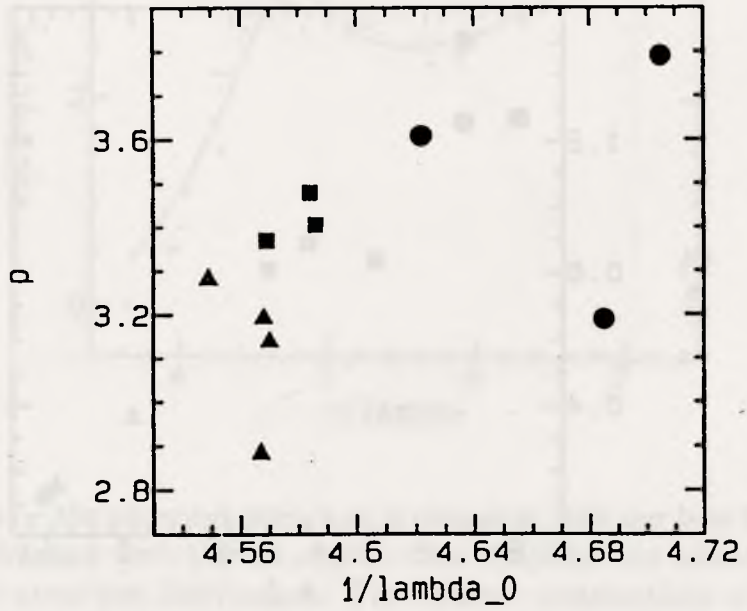


**Figure 14.**
Position of the central wavelength $\lambda_0$ of the 2200Åbump is plotted versus power-law index. Symbols as in Fig. 11.

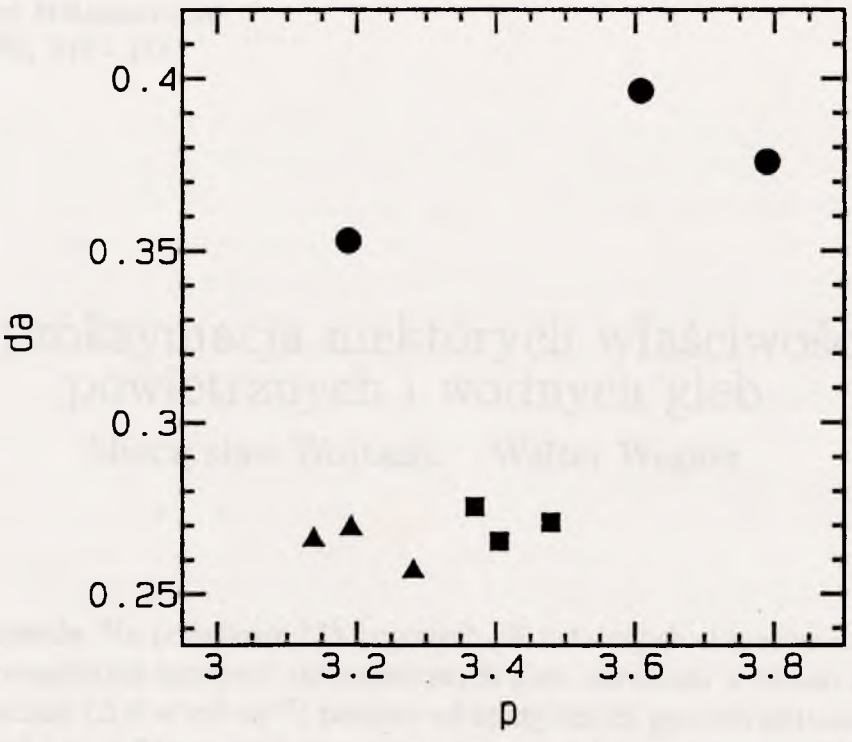


**Figure 15.**
Relation between power-law index and *da* for the stars belonging to three families. Symbols as in Fig. 11.